JOURNAL OF INTEGRAL EQUATIONS
AND APPLICATIONS
Volume 19, Number 3, Fall 2007

FAST METHODS FOR THREE-DIMENSIONAL INVERSE OBSTACLE SCATTERING PROBLEMS

HELMUT HARBRECHT AND THORSTEN HOHAGE

ABSTRACT. We study the inverse problem to reconstruct the shape of a three dimensional sound-soft obstacle from measurements of scattered acoustic waves. To solve the forward problem we use a wavelet based boundary element method and prove fourth order accuracy both for the evaluation of the forward solution operator and its Fréchet derivative. Moreover, we discuss the characterization and implementation of the adjoint of the Fréchet derivative. For the solution of the inverse problem we use a regularized Newton method. The boundaries are represented by a class of parametrizations, which include non star-shaped domains and which are not uniquely determined by the obstacle. To prevent degeneration of the parametrizations during the Newton iteration, we introduce an additional penalty term. Numerical examples illustrate the performance of our method.

1. Introduction. It is well known that the propagation of an acoustic wave in a homogeneous, isotropic and inviscid fluid is approximately described by a velocity potential $U(\mathbf{x}, t)$ satisfying the wave equation $U_{tt} = c^2 \Delta U$. Here, c denotes the speed of sound, $v = U_{\mathbf{x}}$ is the velocity field and $p = -U_t$ is the pressure. For more details on the physical background, we refer the reader to the monograph [**5**]. If U is time harmonic, that is, $U(\mathbf{x}, t) = \mathrm{Re}\,(u(\mathbf{x})e^{-i\omega t})$, $\omega > 0$, in complex notation, then the complex valued space-dependent function u satisfies the Helmholtz equation

$$\Delta u + \kappa^2 u = 0 \text{ in } \mathbf{R}^3 \setminus \overline{\Omega}. \tag{1.1}$$

Here, $\Omega \subset \mathbf{R}^3$ describes an obstacle and $\kappa = \omega/c$ is the wave number. We assume that Ω is bounded, that $\mathbf{R}^3 \setminus \Omega$ is simply connected and that the boundary $\Gamma = \partial\Omega$ is smooth. For sound-soft obstacles the pressure p vanishes on Γ, which leads to the Dirichlet boundary condition

$$u = 0 \text{ on } \Gamma. \tag{1.2}$$

Received by the editors on November 23, 2005, and in revised form on September 13, 2006.

We shall consider the situation that $u = u_i + u_s$ is composed of a known incident plane wave $u_i(\mathbf{x}) = e^{i\kappa \mathbf{d}\cdot\mathbf{x}}$ with direction $\mathbf{d}$ ($\|\mathbf{d}\| = 1$), and a scattered wave u_s. The scattered field satisfies the Sommerfeld radiation condition

$$\lim_{r\to\infty} r\left\{\frac{\partial u_s}{\partial r} - i\kappa u_s\right\} = 0, \quad r = \|\mathbf{x}\|, \tag{1.3}$$

which implies the asymptotic behavior

$$u_s(\mathbf{x}) = \frac{e^{i\kappa\|\mathbf{x}\|}}{\|\mathbf{x}\|}\left\{u_\infty\left(\frac{\mathbf{x}}{\|\mathbf{x}\|}\right) + \mathcal{O}\left(\frac{1}{\|\mathbf{x}\|}\right)\right\}, \quad \|\mathbf{x}\| \to \infty. \tag{1.4}$$

A function which satisfies (1.1) and (1.3) is called a radiating solution to the Helmholtz equation. The function $u_\infty : \mathbf{S}^2 := \{\mathbf{x} : \|\mathbf{x}\| = 1\} \to \mathbf{C}$ is called the far field pattern, which is always analytic, see [**5**].

The direct scattering problem consists in finding u_s as solution to the exterior boundary value problem (1.1)–(1.3), given u_i and Ω. We shall be concerned with the inverse problem to find an approximation of Ω, given u_i and measurement data u_∞^δ of the exact far field pattern u_∞. Here, δ denotes the noise level, which is measured in the $L^2(\mathbf{S}^2)$-norm, i.e., $\|u_\infty^\delta - u_\infty\|_{L^2(\mathbf{S}^2)} \leq \delta$.

The numerical solution of two-dimensional inverse obstacle scattering problems by iterative regularization methods has been studied intensively in the literature, see e.g., [**11, 15, 16, 25, 26, 28**]. On the other hand, we are only aware of the paper by Farhat et al. [**8**] concerning three-dimensional inverse obstacle scattering problems in the resonance region. In [**8**] the forward problem was solved on a 24 processor machine by finite elements using domain decomposition and transparent boundary conditions on the artificial boundary of the computational domain. The number of unknowns can be significantly reduced if boundary element methods are employed, but this leads to a dense system matrix. To cope with this difficulty one may either apply multi-pole and panel clustering methods or wavelet based methods. Whereas in the first class of methods the system matrix is never set up, in the second class of methods the system matrix is computed with respect to a wavelet basis in which it can accurately be approximated by a sparse matrix. Computing the system matrix is comparatively expensive, but then matrix-vector multiplications can be carried out extremely fast. This

is advantageous in the context of Newton-type methods where the same matrix equation has to be solved for a large number of righthand sides.

A particular emphasis of this paper is on the reconstruction of non star-shaped obstacles. Therefore, we start the following section with a discussion of the parametrization of the boundaries of such obstacles. Since the parametrization of the boundary will not be unique, and some parametrizations are preferable to others from a numerical perspective, we introduce an additional penalty term in the regularized Newton method for finding an approximate parametrization of the true obstacle.

In Sections 3 and 4 we describe the wavelet based boundary element method and show that bilinear shape functions lead to fourth order accurate approximations of the forward solution operator F and its Fréchet derivative F'. Moreover, in Section 5 we discuss the characterization and implementation of the adjoint operator $F'[\cdot]^*$ which is needed in our implementation of the Newton method. Finally, in Section 6 we present numerical examples.

2. Parametrization of the boundary and iterative regularization methods. Let $\Gamma_{\text{ref}} \subset \mathbf{R}^3$ be a smooth closed reference surface of the same genus as Γ. (In our numerical examples in Section 6 we will always choose $\Gamma_{\text{ref}} = \mathbf{S}^2$.) Then Γ can be parametrized by a smooth mapping

$$\Psi : \Gamma_{\text{ref}} \longrightarrow \Gamma,$$

which is one-to-one, preserves orientation, and $D\Psi(\mathbf{x})$ is one-to-one for all $\mathbf{x} \in \Gamma_{\text{ref}}$. Here $D\Psi(\mathbf{x}) : T_{\mathbf{x}} \to T_{\Psi(\mathbf{x})}$ denotes the derivative of Ψ at $\mathbf{x}$, which is a linear mapping from the tangent space of Γ_{ref} at $\mathbf{x}$ to the tangent space of Γ at $\Psi(\mathbf{x})$. A linear mapping $L : T_{\mathbf{x}} \to T_{\Psi(\mathbf{x})}$ is called orientation-preserving if $(L\mathbf{a}) \times (L\mathbf{b})$ is an outward pointing normal vector on Γ for all $\mathbf{a}, \mathbf{b} \in T_{\mathbf{x}}$ such that $\mathbf{a} \times \mathbf{b}$ is an outward pointing normal vector on Γ_{ref}. Ψ is called orientation-preserving if $D\Psi(\mathbf{x})$ is orientation-preserving for all $\mathbf{x} \in \Gamma_{\text{ref}}$. The tangent spaces are equipped with an inner product induced by the standard inner product in $\mathbf{R}^3$. If $O : T_{\Psi(\mathbf{x})} \to T_{\mathbf{x}}$ is any orthogonal, orientation-preserving mapping, then $OD\Psi(\mathbf{x})$ maps $T_{\mathbf{x}}$ to itself, and we can define $\det(D\Psi(\mathbf{x})) := \det(OD\Psi(\mathbf{x}))$. It is easy to check that this definition does not depend on the choice of O. If we choose any orthonormal bases $\{\mathbf{a}, \mathbf{b}\}$ in $T_{\mathbf{x}}$ and $\{\mathbf{c}, \mathbf{d}\}$ in $T_{\Psi(\mathbf{x})}$ such that $\mathbf{a} \times \mathbf{b}$ and $\mathbf{c} \times \mathbf{d}$ are

pointing outwards, and if $A \in \mathbf{R}^{2\times 2}$ is the matrix representing $D\Psi(\mathbf{x})$ with respect to these bases, we have $\det(D\Psi(\mathbf{x})) = \det(A)$. With this notation, the transformation formula

$$\int_{\Gamma} f(\mathbf{y})\, d\sigma_{\mathbf{y}} = \int_{\Gamma_{\mathrm{ref}}} f(\Psi(\mathbf{x}))\det(D\Psi(\mathbf{x}))\, d\sigma_{\mathbf{x}} \tag{2.1}$$

holds true for any $f \in C(\Gamma)$.

Since we want to work in a Hilbert space setting, we describe the smoothness of Ψ by a Sobolev space $X := H^s(\Gamma_{\mathrm{ref}}; \mathbf{R}^3)$ with $s > 2$. Let

$$X_{\mathrm{adm}} := \left\{ \Psi \in H^s(\Gamma_{\mathrm{ref}}; \mathbf{R}^3) : \begin{array}{r} \Psi \text{ is one-to-one, orientation-preserving,} \\ \text{and } \det(D\Psi(x)) \neq 0 \text{ for all } x \in \Gamma_{\mathrm{ref}} \end{array} \right\}$$

be the set of admissible parametrizations, let $Y := L^2(\mathbf{S}^2)$ and define the operator

$$F : X_{\mathrm{adm}} \longrightarrow Y, \quad \Psi \mapsto u_\infty, \tag{2.2}$$

which maps a parametrization Ψ to the far field pattern u_∞ corresponding to the obstacle described by Ψ. Thus, the inverse scattering problem can be formulated as an operator equation

$$F(\Psi) = u_\infty^\delta. \tag{2.3}$$

The special case that the obstacle is star-shaped with respect to a known point (without loss of generality, the origin) has been studied extensively in the literature, see [**11, 16, 25, 26, 28**]. In this case it is natural to choose Ψ in the form

$$\Psi(\mathbf{x}) = r(\mathbf{x})\mathbf{x}, \quad \mathbf{x} \in \Gamma_{\mathrm{ref}} = \mathbf{S}^2 \tag{2.4}$$

with a positive scalar function r and define the operator

$$F_{\mathrm{star}} : \widetilde{X}_{\mathrm{adm}} \longrightarrow Y, \quad r \mapsto u_\infty \tag{2.5}$$

on the domain $\widetilde{X}_{\mathrm{adm}} := \{r \in H^s(\mathbf{S}^2; \mathbf{R}) : r > 0\}$.

Whereas the function r in (2.4) is uniquely determined by the obstacle, the parametrization of a surface Γ by elements of X_{adm} is not unique. In fact, if $\Phi \in X_{\text{adm}}$ is any smooth bijective mapping on Γ_{ref}, then $\Psi \circ \Phi$ is another admissible parametrization of Γ. Therefore, F is not one-to-one even if Γ is uniquely determined by u_∞. We will further discuss this problem below.

It can be shown that the operator F is Fréchet differentiable and that the derivative can be characterized by a boundary value problem, see Kirsch [**23**]. More precisely, for $\Psi \in X_{\text{adm}}$ and $\mathbf{V} \in H^s(\Gamma_{\text{ref}}; \mathbf{R}^3)$ the derivative of F at Ψ in direction $\mathbf{V}$ is given by

$$F'[\Psi](\mathbf{V}) = u'_{\mathbf{V},\infty} \tag{2.6}$$

where $u'_{\mathbf{V},\infty}$ is the far field pattern of a solution $u'_{\mathbf{V}}$ to the Helmholtz equation (1.1), which satisfies the Sommerfeld radiation condition (1.3) and the boundary condition

$$u'_{\mathbf{V}} = -(\mathbf{V} \cdot \mathbf{n}) \frac{\partial u}{\partial \mathbf{n}} \text{ on } \Gamma. \tag{2.7}$$

Here and in the sequel, $\mathbf{n}(\mathbf{x})$ denotes the outward normal vector on Ω at $\mathbf{x} \in \Gamma$.

One of the most attractive methods for the solution of nonlinear ill-posed operator equations is the iteratively regularized Gauss-Newton method. The nth step of this method consists in computing an update $\mathbf{V}_n = \Psi_{n+1} - \Psi_n$ by solving the quadratic minimization problem

$$\|F'[\Psi_n]\mathbf{V} + F(\Psi_n) - u_\infty^\delta\|_Y^2 + \alpha_n \|\mathbf{V} + \Psi_n - \Psi_0\|_X^2 = \min!, \quad \mathbf{V} \in H^s(\Gamma_{\text{ref}}; \mathbf{R}^3) \tag{2.8}$$

with regularization parameters α_n which can be chosen of the form $\alpha_n = \alpha_0 q^n$, $q \in (0,1)$. More precisely, we used $q = 2/3$ and chose α_0 such that $\|F'[\Psi_0]\mathbf{V}_0 + F(\Psi_0) - u_\infty^\delta\|_Y \approx 0.8\|F(\Psi_0) - u_\infty^\delta\|_Y$. The convergence of the IRGNM was analyzed by Bakushinskii [**1**], Blaschke, et al. [**2**] and Hohage [**16**]. This analysis (see also the recent monograph [**20**]) also includes the case that F is not one-to-one. In this case the sequence (Ψ_n) converges to a solution with minimal distance to Ψ_0.

In our problem not all parametrizations of a given boundary are equally well suited in a Newton iteration. The derivative $D\Psi(\mathbf{x})$ should

not only be nonsingular for all $\mathbf{x} \in \Gamma_{\mathrm{ref}}$, but the inverse $[D\Phi(\mathbf{x})]^{-1}$ should also be of reasonable size. This is advantageous for the solution of the forward problem by boundary element methods, and it reduces the danger of getting an inadmissible parametrization in the following Newton steps. If $\|D\Phi(\mathbf{x}_0)\|$ is small for some $\mathbf{x}_0 \in \Gamma_{\mathrm{ref}}$, then there exists a small perturbation $\mathbf{V}$ of Φ such that $\Phi+\mathbf{V}$ describes a self-penetrating and hence inadmissable surface near $\mathbf{x}_0$. We typically observed this type of self-penetration already after a few Newton iterations.

Therefore, we introduce a mapping $G : X_{\mathrm{adm}} \to Z$ with values in a Hilbert space Z such that $\|G(\Psi)\|_Z$ is small for desirable parametrizations and include this as an additional penalty term in the Newton iteration:

$$\begin{aligned}(2.9)\quad \|F'[\Psi_n]\mathbf{V} + F(\Psi_n) - u_\infty^\delta\|_Y^2 + \alpha_n\|G'[\Psi_n]\mathbf{V} + G(\Psi_n)\|_Z^2 \\ +\alpha_n\|\mathbf{V} + \Psi_n - \Psi_0\|_X^2 = \min!\end{aligned}$$

To define a possible choice of G, we identify $D\Psi(\mathbf{x}) : T_{\mathbf{x}} \to T_{\Psi(\mathbf{x})}$ with its 3×2 matrix representation using a fixed choice of orthonormal bases of the tangent spaces $T_{\mathbf{x}}$, $\mathbf{x} \in \Gamma_{\mathrm{ref}}$ and the embedding of $T_{\Psi(\mathbf{x})}$ in $\mathbf{R}^3$. Moreover, we denote by $D\Psi(x)^\dagger = (D\Psi(\mathbf{x})^* D\Psi(\mathbf{x}))^{-1} D\Psi(\mathbf{x})^*$ the Moore-Penrose inverse of $D\Psi(\mathbf{x})$ and define the inner product $(A : B) := \sum_{j=1}^m \sum_{k=1}^n a_{jk} b_{jk}$ of $m \times n$ matrices $A = (a_{jk})$ and $B = (b_{jk})$ corresponding to the Frobenius norm $\|A\|_F = (A : A)^{1/2}$. Moreover, we define the Hilbert space $Z := L^2(\Gamma_{\mathrm{ref}}; \mathbf{R}^{3\times 2})$ of square integrable (3×2)-matrix valued functions on Γ_{ref} with inner product

$$\langle A, B\rangle_Z := \int_{\Gamma_{\mathrm{ref}}} A(\mathbf{x}) : B(\mathbf{x})\, d\sigma_{\mathbf{x}},$$

and the operator $G : X_{\mathrm{adm}} \to Z$ by

$$(2.10)\qquad (G(\Psi))(\mathbf{x}) := D\Psi(x)^\dagger, \quad x \in \Gamma_{\mathrm{ref}}.$$

For our problem, it would be computationally very expensive to compute and invert the matrix for $F'[\Psi_n]$. Instead, we solve the minimization problem (2.9) iteratively by the conjugate gradient method. In [**17**] a preconditioning technique was developed for CG iteration applied to (2.8), which keeps $F'[\Psi_m]$ fixed for a number of Newton steps

($m \leq n$). To apply the same technique to (2.9) we use the modified problems

$$\|F'[\Psi_m]\mathbf{V} + F(\Psi_n) - u_\infty^\delta\|_Y^2 + \alpha_m\|G'[\Psi_m]\mathbf{V} + G(\Psi_n)\|_Z^2 \\ +\alpha_n\|\mathbf{V} + \Psi_n - \Psi_0\|_X^2 = \min!$$

or equivalently

$$\left\| \begin{bmatrix} F'[\Psi_m] \\ \sqrt{\alpha_m}G'[\Psi_m] \\ \sqrt{\alpha_n}I \end{bmatrix} \mathbf{V} - \begin{bmatrix} u_\infty^\delta - F(\Psi_n) \\ -\sqrt{\alpha_m}G(\Psi_n) \\ \sqrt{\alpha_n}(\Psi_0 - \Psi_n) \end{bmatrix} \right\|_{Y\times Z\times X}^2 = \min! \tag{2.11}$$

Let us introduce the notation A_m for the operator

$$(F'[\Psi_m], \sqrt{\alpha_m}G'[\Psi_m])^T : X \to Y \times Z.$$

In the mth Newton step ($n = m$) we apply the CG method to the normal equation corresponding to (2.11), i.e., to invert the operator $A_m^*A_m + \alpha_m I$. Memorizing all quantities computed in the CG method, we can then apply the Lanczos algorithm to obtain good approximations to the largest eigenvalues and eigenvectors of $A_m^*A_m + \alpha_m I$. These quantities are used in the following Newton steps to construct a preconditioner which shifts the largest eigenvalues of the matrix $A_m^*A_m + \alpha_n I$ to the cluster at α_n. Therefore, the condition number of the preconditioned system is small, and only a few preconditioned CG steps are required to solve it. For details we refer to [**17**].

3. Boundary integral equations. In this section we review boundary integral equations both for solving the forward scattering problem and for evaluating domain derivatives using a combination of a Green's and a potential ansatz, see [**25**]. In the following

$$E(\mathbf{x}, \mathbf{y}) = \frac{e^{i\kappa\|\mathbf{x}-\mathbf{y}\|}}{4\pi\|\mathbf{x} - \mathbf{y}\|}$$

denotes the fundamental solution to the Helmholtz equation. Adding Green's representation formula for u_s and Green's second theorem in Ω for $E(\mathbf{x}, \cdot)$ and u_i, it can be shown that the total field $u = u_i + u_s$ for Dirichlet boundary conditions satisfies

$$u(\mathbf{x}) + \int_\Gamma \frac{\partial u}{\partial \mathbf{n}}(\mathbf{y})E(\mathbf{x}, \mathbf{y})\, d\sigma_\mathbf{y} = u_i(\mathbf{x}), \quad \mathbf{x} \in \mathbf{R}^3 \setminus \overline{\Omega}. \tag{3.1}$$

We introduce the acoustic single layer potential operator $\mathcal{S}$, its normal derivative $\mathcal{D}'$ and the double layer potential operator $\mathcal{D}$ by

$$\begin{aligned}(\mathcal{S}\rho)(\mathbf{x}) &:= \int_\Gamma E(\mathbf{x},\mathbf{y})\rho(\mathbf{y})\,d\sigma_{\mathbf{y}}, \quad \mathbf{x}\in\Gamma,\\ (\mathcal{D}'\rho)(x) &:= \int_\Gamma \frac{\partial E(\mathbf{x},\mathbf{y})}{\partial \mathbf{n}(\mathbf{x})}\rho(\mathbf{y})\,d\sigma_{\mathbf{y}}, \quad \mathbf{x}\in\Gamma,\\ (\mathcal{D}\rho)(\mathbf{x}) &:= \int_\Gamma \frac{\partial E(\mathbf{x},\mathbf{y})}{\partial \mathbf{n}(\mathbf{y})}\rho(\mathbf{y})\,d\sigma_{\mathbf{y}}, \quad \mathbf{x}\in\Gamma.\end{aligned}$$

Throughout this paper these integral operators will be considered as operators from $L^2(\Gamma)$ to $L^2(\Gamma)$. For jump relations for densities $\rho\in L^2(\Gamma)$ we refer to [**20**]. Letting $\mathbf{x}$ tend to Γ in (3.1) and taking the normal derivative, it can be shown that the Neumann data $\partial u/\partial\mathbf{n}$ of the total field satisfy the integral equation

$$\left(\frac{1}{2}I+\mathcal{D}'-i\eta\mathcal{S}\right)\frac{\partial u}{\partial\mathbf{n}}=\frac{\partial u_i}{\partial\mathbf{n}}-i\eta u_i \ \text{ on } \Gamma, \tag{3.2}$$

for any $\eta\geq 0$. The term involving η has been introduced to ensure unique solvability of the integral equation (3.2). In accordance with Kress [**24**] and Giebermann [**9**] we choose $\eta=\kappa/2$ to obtain a small condition number of the operator on the lefthand side. Letting $\|\mathbf{x}\|$ tend to ∞ in (3.1) we obtain the following formula for the far field pattern of the scattered field:

$$u_\infty(\hat{\mathbf{x}})=-\frac{1}{4\pi}\int_\Gamma e^{-i\kappa\hat{\mathbf{x}}\cdot\mathbf{y}}\frac{\partial u}{\partial\mathbf{n}}(\mathbf{y})\,d\sigma_{\mathbf{y}}, \quad \hat{\mathbf{x}}\in\mathbf{S}^2. \tag{3.3}$$

To compute the derivative $u'_{\mathbf{V}}$ of the scattered field, we make the ansatz

$$u'_{\mathbf{V}}(\mathbf{x})=\int_\Gamma\left(\frac{\partial E(\mathbf{x},\mathbf{y})}{\partial\mathbf{n}(\mathbf{y})}-i\eta E(\mathbf{x},\mathbf{y})\right)\rho(\mathbf{y})\,d\sigma_{\mathbf{y}}, \quad \mathbf{x}\in\mathbf{R}^3\setminus\overline{\Omega}. \tag{3.4}$$

Using the boundary condition (2.7) and the jump relations, this leads to the boundary integral equation

$$\left(\frac{1}{2}I+\mathcal{D}-i\eta\mathcal{S}\right)\rho=-(\mathbf{V}\cdot\mathbf{n})\frac{\partial u}{\partial\mathbf{n}} \ \text{ on } \Gamma. \tag{3.5}$$

The advantage of this ansatz is that the operator on the lefthand side of this equation is the transposed of the operator in (3.2), and the righthand side can easily be computed using the solution of (3.2). A formula for the far field pattern of $u'_{\mathbf{V}}$ is obtained by letting $\|\mathbf{x}\|$ tend to ∞ in (3.4):

$$u'_{\infty,\mathbf{V}}(\hat{\mathbf{x}}) = \frac{1}{4\pi}\int_\Gamma e^{-i\kappa\hat{\mathbf{x}}\cdot\mathbf{y}}(-i\kappa(\mathbf{n}(\mathbf{y})\cdot\hat{\mathbf{x}}) - i\eta)\rho(\mathbf{y})\,d\sigma_{\mathbf{y}}, \quad \hat{\mathbf{x}}\in\mathbf{S}^2. \tag{3.6}$$

4. Wavelet based boundary element methods. We will assume that the boundary manifold Γ is given as a parametric surface consisting of smooth patches. More precisely, let $\square := [0,1]^2$ denote the unit square. The manifold $\Gamma \subset \mathbf{R}^3$ is partitioned into a finite number of *patches*

$$\Gamma = \bigcup_{i=1}^{M}\Gamma_i, \quad \Gamma_i = \gamma_i(\square), \quad i = 1,2,\ldots,M, \tag{4.1}$$

where each $\gamma_i : \square \to \Gamma_i$ defines a diffeomorphism of $\square$ onto Γ_i. The intersection $\Gamma_i \cap \Gamma_{i'}$, $i \neq i'$, of the patches Γ_i and $\Gamma_{i'}$ is assumed to be either $\varnothing$ or a common edge or vertex.

Obviously, it suffices to construct such a parametrization of the reference manifold Γ_{ref}. For the unit sphere $\Gamma_{\mathrm{ref}} = \mathbf{S}^2$ this can be done as follows: The surface of the cube $[-0.5,0.5]^3$ consists of six patches. Each point $\mathbf{x} \in \partial([-0.5,0.5]^3)$ can be lifted onto the boundary Γ via the operation

$$\mathbf{y}(\mathbf{x}) = \Psi\left(\frac{\mathbf{x}}{\|\mathbf{x}\|}\right). \tag{4.2}$$

That way, the surface Γ is subdivided into $M = 6$ patches. This subdivision of the reconstructed surfaces is illustrated in Figure 3 together with further uniform subdivisions of the six patches. The parametric representations $\gamma_i : \Gamma_i \to \Gamma$ can easily be derived from (4.2). Note that the surface of the cube itself cannot serve as reference manifold Γ_{ref} since it is not smooth.

We shall be concerned with the *wavelet Galerkin scheme* for solving the given boundary integral equations (3.2) and (3.5). We consider the

Fredholm integral equation of the second kind

$$Au(\mathbf{x}) = u(\mathbf{x}) + \int_\Gamma k(\mathbf{x},\mathbf{y})u(\mathbf{y})\,d\sigma_{\mathbf{y}} = f(\mathbf{x}), \quad \mathbf{x} \in \Gamma, \tag{4.3}$$

with $A : L^2(\Gamma) \to L^2(\Gamma)$. The crucial ingredient in wavelet methods is a hierarchy of trial spaces $V_j \subseteq V_{j+1} \subseteq L^2(\Gamma)$. Such spaces can be constructed using the parametric representation described above.

We introduce a mesh of level j on the unit square by dyadic subdivisions of depth j into 4^j squares. On this mesh we consider piecewise bilinear nodal basis functions $\{\phi^\square_{j,k} : k \in \Delta^\square_j\}$, where $\Delta^\square_j$ denotes a suitable index set satisfying $|\Delta^\square_j| = (2^j+1)^2$.

We define the set of basis functions on the surface Γ via parametrization

$$\phi_{i,j,k}(\mathbf{x}) := \begin{cases} \phi^\square_{j,k}(\mathbf{s}) & \mathbf{x} = \gamma_i(\mathbf{s}) \in \Gamma_i, \\ 0 & \text{elsewhere,} \end{cases}$$

where $i = 1, 2, \dots, M$. Then, the trial spaces

$$V_j := \operatorname{span}\{\phi_{i,j,k} : (i,k) \in \Delta_j\},$$

where $\Delta_j := \{(i,k) : i = 1, \dots, M, k \in \Delta^\square_j\}$, are nested with respect to j.

The Galerkin formulation of (4.3) reads: find $u_j \in V_j$ such that

$$\langle Au_j, v_j\rangle = \langle f, v_j\rangle \ \text{ for all } \ v_j \in V_j.$$

Equivalently, considering any (stable) basis $\{\xi_{i,j,k} : (i,k) \in \Delta_j\}$ of V_j and making the ansatz $u_j = \sum_{(i,k)\in\Delta_j} [\mathbf{u}^\xi_j]_{(i,k)}\xi_{i,j,k}$, we seek the vector $\mathbf{u}_j \in \mathbf{R}^{|\Delta_j|}$ solving the linear system of equations

$$\mathbf{A}^\xi_j \mathbf{u}^\xi_j = \mathbf{f}^\xi_j, \tag{4.4}$$

where the system matrix respective the load vector are given by

$$[\mathbf{A}^\xi_j]_{(i,k),(i',k')} = (A\xi_{i',j,k'}, \xi_{i,j,k})_{L^2(\Gamma)}, \quad [\mathbf{f}^\xi_j]_{i,k} = \xi_{i,j,k})_{L^2(\Gamma)}. \tag{4.5}$$

Using the *single scale bases* $\{\phi_{i,j,k} : (i,k) \in \Delta_j\}$ we obtain the traditional boundary element method. Then, the system matrix $\mathbf{A}^\phi_j$ is

densely populated and we end up with an at least quadratic complexity for computing the approximate solution of (4.4), i.e., the computational work scales like $\mathcal{O}(|\Delta_j|^2) = \mathcal{O}(16^j)$.

We employ instead appropriate *biorthogonal spline wavelets* $\{\psi_{i,j,k} : (i,k) \in \Delta_j\}$ as constructed in several papers, see e.g., [**7, 12, 14**]. Then, we obtain a quasi-sparse system matrix $\mathbf{A}_j^{\psi}$ having only $\mathcal{O}(|\Delta_j|)$ relevant matrix coefficients. Applying the matrix compression strategy developed in [**6, 27**] combined with an exponentially convergent *hp*-quadrature method [**13**], the wavelet Galerkin scheme produces the approximate solution of (4.3) within linear complexity. However, one has to adopt the bandwidth parameters in the wavelet matrix compression appropriately since the Helmholtz kernel oscillates. It turns out that it is sufficient to increase them proportional to the wave number κ, see [**19**] for the details.

Next, we shall investigate the approximation errors which appear in the iterative solution of (2.3), namely the approximation errors of the far field patterns (3.3) and (3.6) of the scattered field and its derivative.

Theorem 1. *If $\Psi \in X_{\mathrm{adm}}$ is a smooth parametrization of the boundary Γ and $h_j \sim 2^{-j}$ denotes the step width of the Galerkin discretization, then the discretization error in our approximation F_{h_j} of the forward solution operator F satisfies*

$$\|F(\Psi) - F_{h_j}(\Psi)\|_{L^2} = \mathcal{O}(h_j^4)$$

uniformly in j.

Proof. Since the domain Ω is assumed to be smooth, the Neumann data $\partial u/\partial \mathbf{n}$ are contained in $H^2(\Gamma)$ by elliptic regularity theory. Therefore, in accordance with [**6, 27**], the approximate Neumann data computed by the Fredholm integral equation of second kind (3.2) satisfy

$$\left\| \frac{\partial u}{\partial \mathbf{n}} - \left[\frac{\partial u}{\partial n} \right]_{h_j}^{\mathrm{app}} \right\|_{H^t(\Gamma)} \lesssim h_j^{2-t} \left\| \frac{\partial u}{\partial \mathbf{n}} \right\|_{H^2(\Gamma)}, \quad t \in [-2, 0] \tag{4.6}$$

uniformly in j. Now, we consider the far field evaluation (3.3). Since the kernel $-e^{-i\kappa \mathbf{x}\cdot\mathbf{y}}/(4\pi)$ is analytic in $\hat{\mathbf{x}} \in \mathbf{S}^2$ and $\mathbf{y} \in \Gamma$, the integral

operator defined by the righthand side of (3.3), which maps $\partial u/\partial \mathbf{n}$ to u_∞ is bounded from $H^{-2}(\Gamma)$ to $L^2(\mathbf{S}^2)$. Therefore,

$$\|u_\infty - u_{\infty,h_j}^{\mathrm{app}}\|_{L^2(\mathbf{S}^2)} \lesssim \left\| \frac{\partial u}{\partial \mathbf{n}} - \left[\frac{\partial u}{\partial \mathbf{n}}\right]_{h_j}^{\mathrm{app}} \right\|_{H^{-2}(\Gamma)}.$$

This together with (4.6) implies the assertion. □

The corresponding error estimate for the approximation of the Fréchet derivative is a bit more involved:

Theorem 2. *If $\mathbf{V} \in C^2(\Gamma_{\mathrm{ref}}; \mathbf{R}^3)$ in addition to the assumptions of Theorem 1, then the approximation $F'[\Psi]_{h_j}\mathbf{V}$ of the Fréchet derivative satisfies*

$$\|F'[\Psi]\mathbf{V} - F'[\Psi]_{h_j}\mathbf{V}\|_{L^2} = \mathcal{O}(h_j^4)$$

uniformly in j.

Proof. Let $f := -(\mathbf{V}\cdot\mathbf{n})\frac{\partial u}{\partial \mathbf{n}}$ denote the exact righthand side of (3.5) and $f_{h_j}^{\mathrm{app}} := -(\mathbf{V}\cdot\mathbf{n})[\frac{\partial u}{\partial \mathbf{n}}]_{h_j}^{\mathrm{app}}$ its approximation. Using $\mathbf{V}\cdot\mathbf{n} \in C^2(\Gamma)$ and (4.6), we obtain

$$\|f - f_{h_j}^{\mathrm{app}}\|_{H^t(\Gamma)} \lesssim h_j^{2-t}, \quad t \in [-2, 0]. \tag{4.7}$$

Our approximation $\rho_{h_j}^{\mathrm{app}}$ to the solution ρ of (3.5) is defined by

$$\left\langle A\rho_{h_j}^{\mathrm{app}}, \varphi_{h_j}\right\rangle = \left\langle f_{h_j}^{\mathrm{app}}, \varphi_{h_j}\right\rangle \text{ for all } \varphi_{h_j} \in V_j$$

with the integral operator A on the righthand side of (3.5). For any $g \in L^2(\Gamma)$ let $\varphi^g \in L^2(\Gamma)$ denote the solution to the adjoint problem

$$\langle Av, \varphi^g\rangle = \langle g, v\rangle \text{ for all } v \in L^2(\Gamma).$$

Moreover, let $\varphi_{h_j}^g \in V_j$ denote the L^2orthogonal projection of φ^g onto

V_j. Using the definition of the adjoint problem, we obtain

$$\begin{aligned}
\|\rho-\rho_{h_j}^{\mathrm{app}}\|_{H^{-2}(\Gamma)} &= \sup_{\|g\|_{H^2(\Gamma)}\le 1} |\langle g,\rho-\rho_{h_j}^{\mathrm{app}}\rangle| \\
&= \sup_{\|g\|_{H^2(\Gamma)}\le 1} |\langle A(\rho-\rho_{h_j}^{\mathrm{app}}),\varphi^g\rangle| \\
&\le \sup_{\|g\|_{H^2(\Gamma)}\le 1} \{|\langle A(\rho-\rho_{h_j}^{\mathrm{app}}),\varphi^g \\
&\quad -\varphi_{h_j}^g\rangle| + |\langle A(\rho-\rho_{h_j}^{\mathrm{app}}),\varphi_{h_j}^g\rangle|\} \\
&\lesssim \sup_{\|g\|_{H^2(\Gamma)}\le 1} \{\|\rho-\rho_{h_j}^{\mathrm{app}}\|_{L^2(\Gamma)}\|\varphi^g \\
&\quad -\varphi_{h_j}^g\|_{L^2(\Gamma)} + |\langle f-f_{h_j}^{\mathrm{app}},\varphi_{h_j}^g\rangle|\}.
\end{aligned} \tag{4.8}$$

We now estimate the terms on the righthand side of this inequality separately. By the first Strang lemma we have

$$\|\rho-\rho_{h_j}^{\mathrm{app}}\|_{L^2(\Gamma)} \lesssim h_j^2.$$

Moreover,

$$\|\varphi^g-\varphi_{h^j}^g\|_{L^2(\Gamma)} \lesssim h_j^2\|\varphi^g\|_{H^2(\Gamma)} \lesssim h_j^2\|g\|_{H^2(\Gamma)}. \tag{4.9}$$

Here the second inequality follows from the fact the $A^* : H^2(\Gamma) \to H^2(\Gamma)$ is bounded and boundedly invertible, see e.g. Kirsch [**21**]. Finally, the last term can be estimated by

$$\begin{aligned}
|\langle f-f_{h_j}^{\mathrm{app}},\varphi_{h_j}^g\rangle| &\le |\langle f-f_{h_j}^{\mathrm{app}},\varphi_{h_j}^g-\varphi^g\rangle| + |\langle f-f_{h_j}^{\mathrm{app}},\varphi^g\rangle| \\
&\le \|f-f_{h_j}^{\mathrm{app}}\|_{L^2(\Gamma)}\|\varphi_{h_j}^g-\varphi^g\|_{L^2(\Gamma)} \\
&\quad + \|f-f_{h_j}^{\mathrm{app}}\|_{H^{-2}(\Gamma)}\|\varphi^g\|_{H^2(\Gamma)} \\
&\lesssim h_j^4\|g\|_{H^2(\Gamma)}
\end{aligned}$$

using (4.7) and (4.9). Putting the last four inequalities together, we arrive at

$$\|\rho-\rho_{h_j}^{\mathrm{app}}\|_{H^{-2}(\Gamma)} \lesssim h_j^4$$

uniformly in j. Now the proof is finished by applying the last argument of the proof of Theorem 1 to (3.6) instead of (3.3). □

Obviously, the constants in Theorems 1 and 2 hidden in the Landau symbols $\mathcal{O}$ depend on Ψ. In particular, these constants may deteriorate in a Newton iteration, e.g., if $\Psi_n(\Gamma_{\mathrm{ref}})$ approaches a self-penetrating surface or if the mesh on $\Psi_n(\Gamma_{\mathrm{ref}})$ becomes too nonuniform. We try to avoid these effects by the incorporation of the additional penalty term in (2.9).

5. The adjoint of $F'[\Psi]$. Our method is based on iteratively solving the normal equation corresponding to (2.11), which requires repeated application of the adjoint of the Fréchet derivative $F'[\Psi]$, a topic which we now discuss. It can easily be shown using (5.1) below that $F'[\Psi]$ can uniquely be extended to a bounded linear operator $F'[\Psi]_{L^2} : L^2(\Gamma_{\mathrm{ref}};\mathbf{R}^3) \to L^2(\mathbf{S}^2;\mathbf{C})$ for every $\Psi \in X_{\mathrm{adm}}$. Its adjoint will be denoted by $F'[\Psi]^*_{L^2}$. Since $F'[\Psi] = F'[\Psi]_{L^2} J_s$ where $J_s : H_s(\Gamma_{\mathrm{ref}};\mathbf{R}^3) \hookrightarrow L^2(\Gamma_{\mathrm{ref}};\mathbf{R}^3)$ denotes the embedding operator, the relation of $F'[\Psi]^*$ and $F'[\Psi]^*_{L^2}$ is given by

$$F'[\Psi]^* = J_s^* F'[\Psi]^*_{L^2}.$$

Note that $F'[\Psi]$ maps from a real to a complex Hilbert space. To speak of the adjoint we interpret the image space $L^2(\mathbf{S}^2;\mathbf{C})$ as a real Hilbert space with inner product $(u_\infty, v_\infty) := \mathrm{Re} \int_{\mathbf{S}^2} u_\infty \overline{v_\infty}\, d\sigma$. In the following we will silently interpret other complex Hilbert spaces as real Hilbert spaces in the same manner. Note that, for a bounded linear mapping $A : H_1 \to H_2$ between complex Hilbert spaces H_1 and H_2, the adjoint of A is the same whether we interpret H_1 and H_2 as real or as complex Hilbert spaces.

We now discuss the implementation of the operator J_s^* if Γ_{ref} is the unit sphere $\mathbf{S}^2$. Recall that the norm in $H^s(\mathbf{S}^2;\mathbf{R}^3)$ can be defined by

$$\|\Psi\|^2_{H_s} = \sum_{n=0}^{\infty} \sum_{m=-n}^{n} (1+n^2)^s \left| \int_{\mathbf{S}^2} \Psi \overline{Y_{n,m}}\, ds \right|_2^2$$

in terms of the spherical harmonics $Y_{n,m}$, see e.g., [**5**]. Hence,

$$J_s^* \Psi = \sum_{n=0}^{\infty} \sum_{m=-n}^{n} (1+n^2)^{-s} \int_{\mathbf{S}^2} \Psi \overline{Y_{n,m}}\, ds\, Y_{n,m}.$$

This is easy to implement since we use the spherical harmonics as basis functions. By the formula (2.7) the operator $F'[\Psi]_{L^2}$ can be factorized as follows:

$$F'[\Psi]_{L^2} = G_\Psi A_\Psi. \tag{5.1}$$

Here $A_\Psi : L^2(\Gamma_{\rm ref}; \mathbf{R}^3) \to L^2(\Gamma; \mathbf{C})$ is defined by

$$(A_\Psi \mathbf{V})(\mathbf{y}) := -\frac{\partial u}{\partial \mathbf{n}}(\mathbf{y}) \mathbf{V}(\Psi^{-1}(\mathbf{y})) \cdot \mathbf{n}(\mathbf{y}), \quad \mathbf{y} \in \Gamma,$$

and $G_\Psi : L^2(\Gamma; \mathbf{C}) \to L^2(\mathbf{S}^2; \mathbf{C})$ is the operator which maps Dirichlet data $f \in L^2(\Gamma)$ to the far field pattern v_∞ of the radiating solution v to the Helmholtz equation satisfying the Dirichlet condition $v = f$ on Γ. It follows from (5.1) that

$$F'[\Psi]^*_{L^2} = A^*_\Psi G^*_\Psi. \tag{5.2}$$

Therefore, we have to characterize the operators G^*_Ψ and A^*_Ψ. A characterization of G^*_Ψ has been obtained by Kirsch [**22**]. We will give another proof of this result corresponding to our implementation of this operator for reasons to be discussed below.

Theorem 3. (1) *Let*

$$v_i^g(\mathbf{y}) := \frac{1}{4\pi} \int_{\mathbf{S}^2} e^{-i\kappa \hat{\mathbf{x}} \cdot \mathbf{y}} g(\hat{\mathbf{x}})\, d\sigma_{\hat{\mathbf{x}}}, \quad \mathbf{y} \in \mathbf{R}^3 \tag{5.3}$$

denote the Herglotz wave function with kernel $g \in L^2(\mathbf{S}^2)$, and let v_g be the total field corresponding to v_i^g as incident field, i.e., $v^g = v_i^g + v_s^g$ where $v = 0$ on Γ and v_s^g is a radiating solution to the Helmholtz equation. Then

$$G^*_\Psi g = \overline{\frac{\partial v^{\bar g}}{\partial \mathbf{n}}}. \tag{5.4}$$

(2) *The adjoint of A_Ψ applied to a function $f \in L^2(\Gamma; \mathbf{C})$ is given by*

$$(A^*_\Psi f)(\mathbf{x}) = -\mathrm{Re}\left(f(\mathbf{y}) \cdot \overline{\frac{\partial u}{\partial \mathbf{n}}(\mathbf{y})} \right) \mathbf{n}(\mathbf{y}) \det(D\Psi(\mathbf{x})), \quad \mathbf{x} \in \Gamma_{\rm ref} \tag{5.5}$$

where $\mathbf{y} := \Psi(x)$.

Proof. (1) If the righthand side of (3.6) is denoted by $(B\rho)(\hat{\mathbf{x}})$ with $B : L^2(\Gamma;\mathbf{C}) \to L^2(\mathbf{S}^2;\mathbf{C})$, then

$$G_\Psi = B\left(\frac{1}{2}I + \mathcal{D} - i\eta S\right)^{-1}. \tag{5.6}$$

We denote the adjoint of an integral operator T by T^* and the transposed by T', i.e., $T'g = \overline{T^*\bar{g}}$. Then

$$G_\Psi^* g = \left(\frac{1}{2}I + \mathcal{D}^* - (i\eta S)^*\right)^{-1} B^* g = \overline{\left(\frac{1}{2}I + \mathcal{D}' - i\eta S'\right)^{-1} B'\bar{g}}. \tag{5.7}$$

We obtain immediately from the definitions (3.6) and (5.3) that

$$B'\bar{g} = \frac{\partial v_i^{\bar{g}}}{\partial \mathbf{n}} - i\eta v_i^{\bar{g}}.$$

Now (5.4) follows from (3.2).

(2) Let $f \in L^2(\Gamma;\mathbf{C})$ and $\mathbf{V} \in L^2(\Gamma_{\mathrm{ref}};\mathbf{R}^3)$. Then

$$\begin{aligned}
&\mathrm{Re}\int_\Gamma f(\mathbf{y})\overline{(A\mathbf{V})(\mathbf{y})}\,d\sigma_{\mathbf{y}} \\
&= -\mathrm{Re}\int_\Gamma f(\mathbf{y})\overline{\frac{\partial u}{\partial \mathbf{n}}(\mathbf{y})}\mathbf{V}(\Psi^{-1}(\mathbf{y}))\cdot\mathbf{n}(\mathbf{y})\,d\sigma_{\mathbf{y}} \\
&= \int_{\Gamma_{\mathrm{ref}}}\left\{-\mathrm{Re}\left(f(\Psi(\mathbf{x}))\cdot\overline{\frac{\partial u}{\partial \mathbf{n}}(\Psi(\mathbf{x}))}\right)\mathbf{n}\Psi(\mathbf{x})\det(D\Psi(\mathbf{x}))\right\}\cdot\mathbf{V}(x)\,d\sigma_{\mathbf{x}}
\end{aligned}$$

by the transformation formula (2.1). This implies (5.5). □

For the performance of the inner CG iteration in the Newton method it is essential that the operators $F'[\Psi]$ and $F'[\Psi]^*$ are discretized in such a way that the discrete operators are adjoint to each other. Since the factorization (5.6) describes our implementation of G_Ψ, we have to replace the operators in the factorization (5.7) of G_Ψ^* by the adjoints of the corresponding matrices described in Section 3. The same holds true for the discretization of the adjoint of A_Ψ using (5.5). If the inversion of the boundary integral operators is done approximately by an iterative method, the solution of the discrete equation systems should be computed to high accuracy.

We now consider star-shaped domains described by parametrizations of the form (2.4). In $\mathbf{R}^2$ the adjoint of the Fréchet derivative for star-shaped obstacles was characterized by Hanke, Hettlich and Scherzer [**11**]. To show the connection to this result and explain the different powers of the radial function r, we formulate the following corollary for arbitrary space dimensions $d \geq 2$:

Corollary 4. *The adjoint of the Fréchet derivative $F'_{\text{star}}[r]$ of the solution operator F_{star} for star-shaped obstacles defined in* (2.5) *is given by*

$$(F'_{\text{star}}[r]^* g)(\mathbf{x}) = -r(\mathbf{x})^{d-1} Re\left(\overline{\frac{\partial v^{\bar{g}}}{\partial \mathbf{n}}(\Psi(\mathbf{x}))} \cdot \overline{\frac{\partial u}{\partial \mathbf{n}}(\Psi(\mathbf{x}))}\right), \quad \mathbf{x} \in \mathbf{S}^{d-1}. \tag{5.8}$$

Proof. In analogy to (5.1) the Fréchet derivative can be decomposed into $F'_{\text{star}}[r]h = G_\Psi \tilde{A}_r$ with the operator $\tilde{A}_r : L^2(\mathbf{S}^2; \mathbf{R}) \to L^2(\Gamma; \mathbf{C})$ defined by

$$(\tilde{A}_r h)(r(\mathbf{x})\mathbf{x}) := -\frac{\partial u}{\partial \mathbf{n}}(\Psi(\mathbf{x}))h(\mathbf{x})\{\mathbf{x} \cdot \mathbf{n}(\Psi(\mathbf{x}))\}, \quad \mathbf{x} \in \mathbf{S}^{d-1}.$$

For a fixed $x \in \mathbf{S}^{d-1}$ we introduce an orthonormal system $\{\mathbf{v}_1, \ldots, \mathbf{v}_{d-1}\}$ of $T_{\mathbf{x}}$ and denote by ∂_j the derivative in the direction $\mathbf{v}_j$. Note that $\mathbf{v}_j = \partial_j \mathbf{x}$. By $\operatorname{Grad} r := \sum_{j=1}^{d-1} \partial_j r \mathbf{v}_j$ we denote the surface gradient of r. Then the normal vector is given by

$$\mathbf{n}(\Psi(\mathbf{x})) = (r(\mathbf{x})^2 + \|\operatorname{Grad} r(\mathbf{x})\|_2^2)^{-1/2}(r(\mathbf{x})\mathbf{x} - \operatorname{Grad} r(\mathbf{x}))$$

since

$$\begin{aligned} \partial_j \Psi(y) \cdot (r(\mathbf{x})\mathbf{x} - \operatorname{Grad} r(\mathbf{x})) & \\ &= (\partial_j r(\mathbf{x})\mathbf{x} + r(\mathbf{x})\mathbf{v}_j) \cdot (r(\mathbf{x})\mathbf{x} - \operatorname{Grad} r(\mathbf{x})) \\ &= \partial_j r(\mathbf{x}) r(\mathbf{x}) - r(\mathbf{x}) \partial_j r(\mathbf{x}) = 0 \end{aligned}$$

for $j = 1, \ldots, d-1$. To compute $\det(D\Psi(\mathbf{x}))$ we consider the augmented mapping $B_{\mathbf{x}} : \mathbf{R}^d \to \mathbf{R}^d$ defined by $B_{\mathbf{x}}\mathbf{x} := \mathbf{n}(\mathbf{x})$ and

$B\mathbf{v}_j := \mathbf{v}_j$ for $j = 1, \dots, d-1$ and note that $\det(D\Psi(\mathbf{x})) = \det(B)$. Hence, using the orthonormal basis $\{\mathbf{x}, \mathbf{v}_1, \dots \mathbf{v}_{d-1}\}$ we obtain

$$\begin{aligned}\det(D\Psi(\mathbf{x})) &= \frac{1}{\sqrt{r(\mathbf{x})^2 + \|\operatorname{Grad} r(\mathbf{x})\|_2^2}} \\ &\quad \times \begin{bmatrix} r(\mathbf{x}) & \partial_1 r(\mathbf{x}) & \cdots & \partial_{d-1} r(\mathbf{x}) \\ -\partial_1 r(x) & r(\mathbf{x}) & 0 & \\ \vdots & & \ddots & \\ -\partial_{d-1} r(\mathbf{x}) & 0 & r(\mathbf{x}) & \end{bmatrix} \\ &= \sqrt{r(\mathbf{x})^2 + \|\operatorname{Grad} r(\mathbf{x})\|_2^2}\, r(\mathbf{x})^{d-2}.\end{aligned}$$

Using (5.5) (which holds true for any $d = 2, 3, \dots$) we obtain

$$\begin{aligned}(\tilde{A}_r^* f)(\mathbf{x}) &= -\operatorname{Re}\left(f(\mathbf{y}) \cdot \overline{\frac{\partial u}{\partial \mathbf{n}}(\Psi(\mathbf{x}))} \right) \\ &\quad \times \{\mathbf{x} \cdot \mathbf{n}(\Psi(\mathbf{x}))\} \det(D\Psi(\mathbf{x})) \\ &= -\operatorname{Re}\left(f(\Psi(\mathbf{x})) \cdot \overline{\frac{\partial u}{\partial \mathbf{n}}(\mathbf{y})} \right) r(\mathbf{x})^{d-1}, \quad \mathbf{x} \in \mathbf{S}^{d-1}.\end{aligned}$$

Together with (5.4) we obtain the assertion. □

6. Numerical results. Our first test is concerned with the reconstruction of a star-shaped domain shown in Figure 1 using the operator F_{star} defined in (2.5). The diameter of the obstacle is roughly 2.8. In two of the experiments the data consisted of six far field patterns corresponding to plane incident waves from top, bottom, right, left, front, and back. A comparison of the results for $\kappa = 4$ and $\kappa = 1$ shows that the quality of the reconstructions is very sensitive to the size of the wave number. The reconstruction for $\kappa = 4$ is surprisingly good considering the fact that the problem is (asymptotically!) exponentially ill-posed. In the bottom left picture, where only one incident wave from top was used, the reconstruction is poor on the shadow side of the obstacle.

In all cases the unit ball was used as an initial guess. The reconstruction in the top right picture was obtained in nine preconditioned Newton steps after 21 minutes computation time on a PC. The radial functions describing the reconstructions belonged to the space of

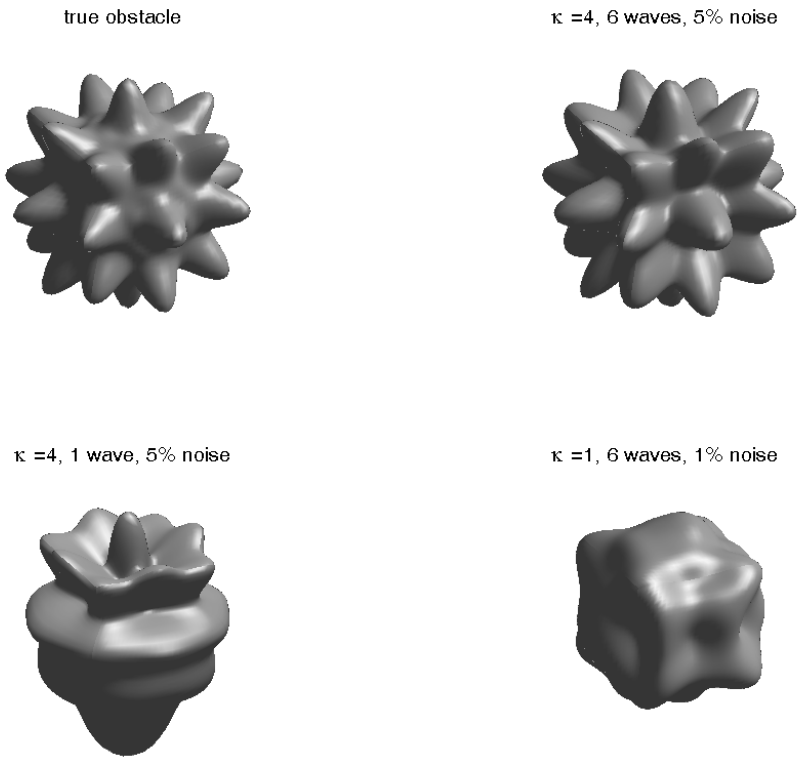

FIGURE 1. Reconstruction of a star-shaped obstacle.

spherical harmonics of order ≤ 20 resulting in $20^2 = 400$ degrees of freedom. To avoid an inverse crime, we chose an obstacle which does not belong to the ansatz space and used a potential ansatz with a finer discretization to compute synthetic data.

In a second test we studied the reconstruction of a dolphin-shaped scatterer. This scatterer is not star-shaped, and we used the operator F defined in (2.2). The surface of the obstacle was given by a triangulation shown at the bottom of Figure 2, which we refined to generate synthetic data. Each Cartesian component of the parametrizations of the reconstructed surfaces was represented by spherical harmonics of order ≤ 20 resulting in $3 \cdot 20^2 = 1200$ unknown design parameters. As an initial guess we used a sphere of diameter 1 shown at the top of

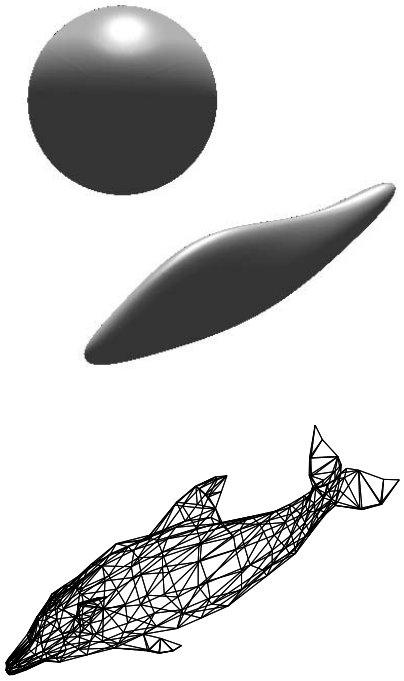

FIGURE 2. Reconstruction of a dolphin with six incident waves with wave number $\kappa = 2$ and 1% noise. Top: initial guess (a ball of radius 0.5) and reconstruction. Bottom: true obstacle.

Figure 2, which has an empty intersection with the true scatterer. To obtain a coarse approximation from a bad initial guess, we found the Newton-CG method, see [**10**], the fastest and most reliable. To obtain more accurate reconstructions given a sufficiently good initial guess, a preconditioned Newton method is more efficient. The reconstruction shown in Figure 2 was obtained in 10 Newton-CG steps after only 6 minutes of computation time. We did not need a step length control for the Newton iteration in this example.

For the computations with wave number $\kappa = 8$ shown in Figure 3 we used the result for $\kappa = 2$ as an initial guess. The result was obtained after six preconditioned Newton steps and 75 minutes computation time on a PC. To solve the forward problems we used the grid shown in Figure 3 corresponding to $6 \cdot (16+1)^2 = 1734$ bilinear basis functions.

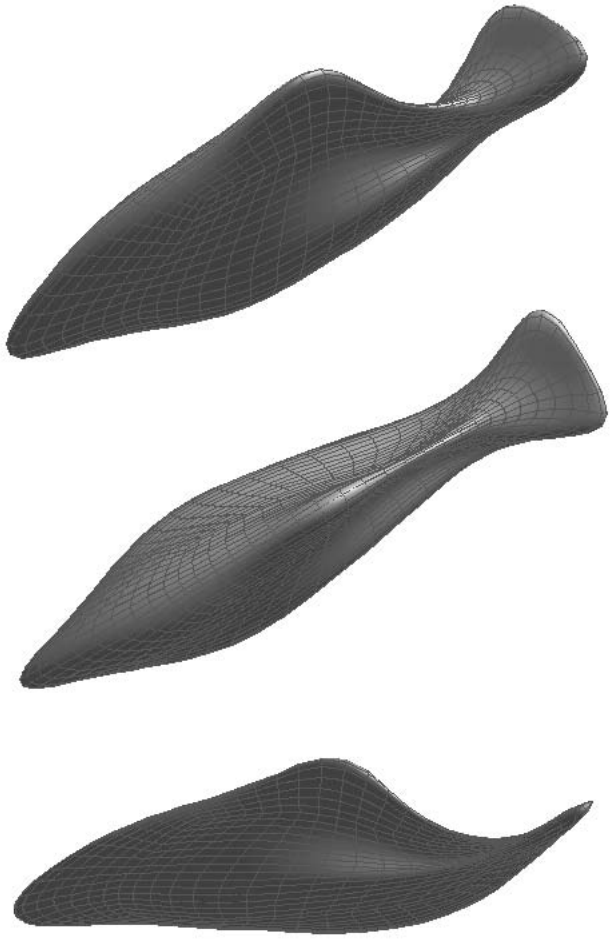

FIGURE 3. Reconstruction of a dolphin with six incident waves with wave number $\kappa = 8$ and 1% noise.

Finally, we comment on the effect of the choice of the parametrization and the penalty terms in (2.9). Figure 3 shows that our scheme automatically leads to an anisotropic mesh refinement in directions of large curvature. This is due to the penalty term $\|\mathbf{V}+\Psi_n-\Psi_0\|_X^2$ in (2.9) since a parametrization of given surface has small second derivatives if it varies slowly in directions of large curvature. This is a desirable effect both for the accurate solution of the forward problems and for the accurate approximation of the geometry using a limited number of degrees of freedom on the unit sphere.

Without the additional penalty term involving the operator G the meshes often deteriorate leading to self-penetrations. The operator G in (2.10) was scaled such that both penalty terms are of the same size at the initial guess. As an alternative to incorporating G in the Newton scheme we also tried to perform a remeshing every few Newton steps. However, this strategy did not turn out to be successful since a remeshing increases the penalty term $\|\mathbf{V} + \Psi_n - \Psi_0\|_X^2$, and in the next Newton step the residual $\|F(\Psi_n) - u_\infty^\delta\|_Y$ tends to increase considerably. This leads to a stagnation or a significant slowdown of the convergence of the Newton iteration.

We finally mention that our choice (2.10) of G only protects against local, but not against global self-penetrations. Therefore, different choices of G may be a subject of further studies.

REFERENCES

1. A.B. Bakushinskii, *The problem of the convergence of the iteratively regularized Gauss-Newton method*, Comput. Math. Math. Phys. **32** (1992), 1353–1359.

2. B. Blaschke, A. Neubauer and O. Scherzer, *On convergence rates for the iteratively regularized Gauss-Newton method*, IMA J. Numerical Anal. **17** (1997), 421–436.

3. H. Brackhage and P. Werner, *Über das Dirichletsche Außenraumproblem für die Helmholtzsche Schwingungsgleichung*, Arch. Math. **16** (1965), 325–329.

4. D. Colton and R. Kress, *Integral equation methods in scattering theory*, in *Pure and applied mathematics*, Chichester, Wiley, New York, 1983.

5. ———, *Inverse acoustic and electromagnetic scattering*, 2nd Edition, Springer Verlag, Berlin, 1997.

6. W. Dahmen, H. Harbrecht and R. Schneider, *Compression techniques for boundary integral equations–optimal complexity estimates*, SIAM J. Numer. Anal. **43** (2006), 2251–2271.

7. W. Dahmen, A. Kunoth and K. Urban, *Biorthogonal spline-wavelets on the interval–stability and moment conditions*, Appl. Comp. Harm. Anal. **6** (1999), 259–302.

8. C. Farhat, R. Tezaur and R. Djellouli, *On the solution of three-dimensional inverse obstacle acoustic scattering problems by a regularized Newton method*, Inverse Problems **18** (2002), 1229–1246.

9. K. Giebermann, *Schnelle Summationsverfahren zur numerischen Lösung von Integralgleichungen für Streuprobleme im* R3, Ph.D. thesis, Universität Karlsruhe, Germany, 1997.

10. M. Hanke, F. Hettlich and O. Scherzer, *The Landweber iteration for an*

inverse scattering problem, in *Proc.* 1995 *Design Engineering Technical Conferences* Vol. 3 Part C, K.W. Wang et al., eds., ASME, New York, 1995.

11. M. Hanke, *Regularizing properties of a truncated Newton–CG algorithm for nonlinear inverse problems*, Numer. Funct. Anal. Optim. **18** (1997), 971–993.

12. H. Harbrecht, *Wavelet Galerkin schemes for the boundary element method in three dimensions*, Ph.D. thesis, Technische Universität Chemnitz, Germany, 2001.

13. H. Harbrecht and R. Schneider, *Wavelet Galerkin schemes for boundary integral equations–implementation and quadrature*, SIAM J. Sci. Comput. **27** (2006), 1347–1370.

14. ———, *Biorthogonal wavelet bases for the boundary element method*, Math. Nach. **269–270** (2004), 167–188.

15. F. Hettlich and W. Rundell, *A second degree method for nonlinear ill-posed problems*, SIAM J. Numer. Anal. **37** (2000), 587–620.

16. T. Hohage, *Logarithmic convergence rates of the iteratively regularized Gauss-Newton method for an inverse potential and an inverse scattering problem*, Inverse Problems **13** (1997), 1279–1299.

17. ———, *On the numerical solution of a three-dimensional inverse medium scattering problem*, Inverse Problems **17** (2001), 1743–1763.

18. ———, *Iterative methods in inverse obstacle scattering: Regularization theory of linear and nonlinear exponentially ill-posed problems*, Ph.D. thesis, JohannesKeplerUniversität Linz, Austria, 1999.

19. D. Huybrechs, J. Simoens and S. Vandewalle, *A note on wave number dependence of wavelet matrix compression for integral equations with oscillatory kernel*, J. Comput. Appl. Math. **172** (2004), 233–246.

20. B. Kaltenbacher, A. Neubauer, and O. Scherzer, *Iterative regularization methods for nonlinear ill-posed problems*. Kluwer, Dordrecht, 2005. to appear.

21. H. Kersten, *Grenz- und Sprungrelationen für Potentiale mit quadrat-summierbarer Dichte*, Resultate d. Math. **3** (1980), 17–24.

22. A. Kirsch, *Surface gradients and continuity properties for some integral operators in classical scattering theory*, Math. Meth. Appl. Sci. **11** (1989), 789–804.

23. ———, *Properties of far field operators in acoustic scattering*, Math. Meth. Appl. Sci. **11** (1989), 773–787.

24. ———, *The domain derivative and two applications in inverse scattering theory*, Inverse Problems **9** (1993), 81–96.

25. R. Kress, *Minimizing the condition number of boundary integral operators in acoustic and electromagnetic scattering*, Quart. J. Mech. Appl. Math. **38** (1985), 323–341.

26. ———, *A Newton method in inverse obstacle scattering*, in *Inverse problems in engineering mechanics*, Bui et al., eds., Balkema, Rotterdam, 1994.

27. R.D. Murch, D.G.H. Tan and D.J.N. Wall, *Newton-Kantorovich method applied to two-dimensional inverse scattering for an exterior Helmholtz problem*, Inverse Problems **4** (1988), 1117–1128.

28. R. Schneider, *Multiskalen- und WaveletMatrixkompression: Analysisbasierte Methoden zur Lösung großer vollbesetzter Gleichungssyteme*, B.G. Teubner, Stuttgart, 1998.

29. W. Tobocman, *Inverse acoustic wave scattering in two dimensions from impenetrable targets*, Inverse Problems **5** (1989), 1131–1144.

Institut für Informatik und Praktische Mathematik, Christian-Albrechts-Universität zu Kiel, Olshausenstr. 40, 24098 Kiel, Germany
Email address: hh@numerik.uni-kiel.de

Institut für Numerische und Angewandte Mathematik, Georg-August-Universität Göttingen, Lotzestr. 1618, 37083 Göttingen, Germany
Email address: hohage@math.uni-goettingen.de